

Controlling Er–Tm interaction in Er and Tm codoped silicon-rich silicon oxide using nanometer-scale spatial separation for efficient, broadband infrared luminescence

Se-Young Seo and Jung H. Shin

Citation: *Appl. Phys. Lett.* **85**, 4151 (2004); doi: 10.1063/1.1812578

View online: <http://dx.doi.org/10.1063/1.1812578>

View Table of Contents: <http://apl.aip.org/resource/1/APPLAB/v85/i18>

Published by the [American Institute of Physics](http://www.aip.org).

Additional information on *Appl. Phys. Lett.*

Journal Homepage: <http://apl.aip.org/>

Journal Information: http://apl.aip.org/about/about_the_journal

Top downloads: http://apl.aip.org/features/most_downloaded

Information for Authors: <http://apl.aip.org/authors>

ADVERTISEMENT



Goodfellow
metals • ceramics • polymers • composites
70,000 products
450 different materials
small quantities fast

www.goodfellowusa.com

Controlling Er–Tm interaction in Er and Tm codoped silicon-rich silicon oxide using nanometer-scale spatial separation for efficient, broadband infrared luminescence

Se-Young Seo^{a)} and Jung H. Shin

*Department of Physics, Korea Advanced Institute of Science and Technology (KAIST),
373-1 Guseong-dong, Yuseong-gu, Daejeon, Korea*

(Received 23 July 2004; accepted 13 September 2004)

The effect of nanometer-scale spatial separation between Er³⁺ and Tm³⁺ ions in Er and Tm codoped silicon-rich silicon oxide (SRSO) films is investigated. Er and Tm codoped SRSO films, which consist of nanocluster Si (nc-Si) embedded inside SiO₂ matrix, were fabricated with electron cyclotron resonance-plasma enhanced chemical vapor deposition of SiH₄ and O₂ with concurrent sputtering of Er and Tm metal targets. Spatial separation between Er³⁺ and Tm³⁺ ions was achieved by depositing alternating layers of Er- and Tm-doped layers of varying thickness while keeping the total film thickness the same. The films display broadband infrared photoluminescence (PL) from 1.5 to 2.0 μm under a single source excitation due to simultaneous excitation of Er³⁺ and Tm³⁺ ions by nc-Si. Increasing the layer thickness from 0 to 72 nm increases the Er³⁺ PL intensity nearly 50-fold while the Tm³⁺ PL intensity is unaffected. The data are well-explained by a model assuming a dipole–dipole interaction between excited Er³⁺ and Tm³⁺ ions, and suggest that by nanoscale engineering, efficient, ultrabroadband infrared luminescence can be obtained in an optically homogeneous material using a single light source. © 2004 American Institute of Physics.
[DOI: 10.1063/1.1812578]

Rare-earth (RE) doping of nanocluster Si (nc-Si) has attracted a great attention as a promising way to create a material base for silicon-compatible photonics.¹ A particular advantage RE-doped nc-Si is that the excitation of RE ions occurs predominantly through an Auger-type interaction between carriers in nc-Si and the RE ions.^{2–5} This leads to strong enhancement of the effective excitation cross section of RE ions, since the absorption cross section of nc-Si is orders of magnitude larger than that of RE ions.^{6–8} Furthermore, since only photocarrier generation is necessary for RE excitation, a low-cost light source such as a light emitting diode can be used to achieve optical gain instead of an expensive laser tuned to the specific absorption band of and RE ion.⁹

An important consequence of such nonresonant excitation process is the ability to excite multiple RE ions with a single pump source. Recently, we have demonstrated that by using Er and Tm codoped silicon-rich silicon oxide (SRSO), which consists of nanocluster Si (nc-Si) embedded inside SiO₂ matrix, broadband infrared luminescence from 1.5 to 2.0 μm due to superposition of Er³⁺ $^4I_{13/2} \rightarrow ^4I_{15/2}$ and Tm³⁺ $^4F_4 \rightarrow ^4H_6$ 4f transitions can be obtained using only a single pump source instead of several lasers tuned to absorption bands of each RE ions.¹⁰ As the luminescence range covers nearly the entire low-loss window of silica optical fibers, this result suggests that compact, low-cost, ultrawideband optical amplifiers that can overcome the bandwidth limitation of conventional optical amplifiers may be obtained using such Er–Tm codoped SRSO.

Unfortunately, such codoping was found to result in a strong reduction of the Er³⁺ luminescence efficiency due to resonant energy transfer from the Er³⁺: $^4I_{13/2}$ state to the

Tm³⁺: 3H_4 state.¹⁰ Such energy transfer is highly unfavorable to photonic applications, yet is difficult to remove in a homogeneous mixture of Er and Tm due to the resonant nature of the interaction. In this letter, we report on controlling the Er–Tm interaction via nanometer (nm)-scale spatial separation. We find that by separating Er³⁺ and Tm³⁺ ions into nm-thin layers, it is possible to reduce the interaction strength and increase the Er³⁺ photoluminescence (PL) intensity nearly 50-fold. The data are well-explained by a model assuming a dipole–dipole interaction between excited Er³⁺ and Tm³⁺ ions, and suggest that by such nanoscale engineering, efficient, ultrabroadband infrared luminescence can be obtained in an optically homogeneous material using a single light source.

SRSO films with 35 at. % Si were deposited on Si(100) wafer using electron cyclotron resonance plasma-enhanced chemical vapor deposition of SiH₄ and O₂. During deposition, Er and Tm metal targets were sputtered in an alternating sequence, thereby creating alternating layers of Er- and Tm-doped SRSO. The total film thickness was kept at 720 nm, while the individual layer thickness, *d*, was varied from 2 to 72 nm. Postdeposition rapid thermal anneal of 5 min at 950 °C in an Ar atmosphere was used to precipitate nc-Si and activate RE ions. Rutherford backscattering spectroscopy and secondary ion mass spectroscopy indicated that Er and Tm ions were doped uniformly in each layers, and well isolated from each other at concentrations of 0.12 and 0.2 at. % for Er and Tm, respectively (data not shown). A schematic description of the film structure is given in Fig. 1. For a comparison, a SRSO film codoped homogeneously with Er and Tm and another doped with Er only were also prepared with the same Si and RE content. The 488 nm line of an Ar ion laser with a nominal power of 600 mW was used for optical excitation source. We note that even though the 488 nm pump light can be absorbed resonantly by Er³⁺,

^{a)}Electronic mail: seyoungseo@kaist.ac.kr

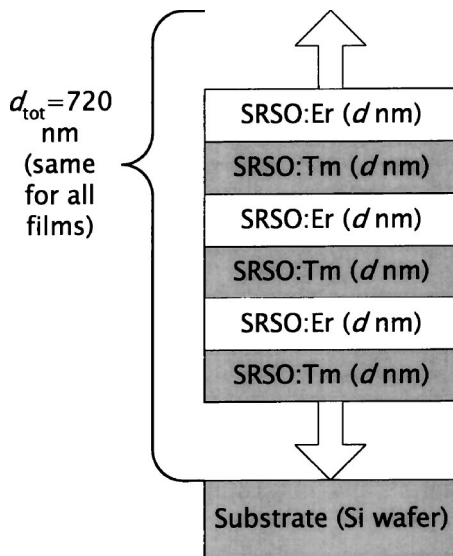


FIG. 1. Schematic description of structure of Er–Tm alternately doped SRSO film.

excitation of Er^{3+} is still dominated by nc-Si. PL spectra were measured at room temperature using either a standard or a long wavelength enhanced InGaAs PIN photodiode, a grating monochromator, and the standard lock-in technique. All spectra are corrected for the system response. Time resolved PL decay traces were recorded using a mechanical chopper and a digitizing oscilloscope. The system response was $180 \mu\text{s}$.

Figure 2 shows the PL spectra of SRSO films with alternating Er- and Tm-doped layers. Also shown is for comparison is the PL spectrum from the film codoped homogeneously with Er and Tm. We observe a broad luminescence peak from 1.5 to $2.0 \mu\text{m}$ due to superposition of ${}^4I_{13/2} \rightarrow {}^4I_{15/2}$ Er^{3+} peak at $1.54 \mu\text{m}$ and ${}^4F_4 \rightarrow {}^4H_6$ Tm^{3+} peak at $1.78 \mu\text{m}$. However, the Er^{3+} peak from the homogeneously doped film is extremely small compared to that of Tm^{3+} . Separating Er and Tm into 2 nm thin layers results in more than tenfold increase in the Er^{3+} PL intensity. Further increasing the layer thickness to 72 nm results in additional fourfold increase in the Er^{3+} PL intensity such that it is about 50 times greater than that from the homogeneously doped film. However, the Tm^{3+} PL intensity is completely unaffected in all cases. The dependence of Er^{3+} and Tm^{3+} PL intensity on the layer thickness is summarized in the inset.

Figure 3 shows time resolved PL decay traces at $\lambda = 1.54 \mu\text{m}$. For comparison, the decay trace of a SRSO film

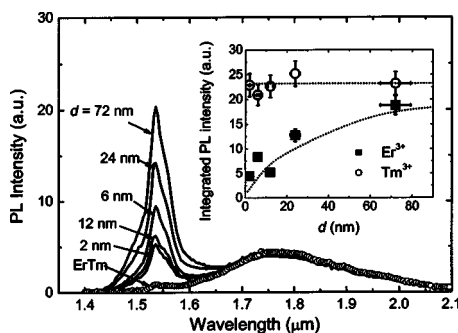


FIG. 2. Infrared PL spectra of Er–Tm alternately doped SRSO film. The inset shows deconvoluted Er^{3+} and Tm^{3+} PL intensity. Dotted lines are a guide for the eyes.

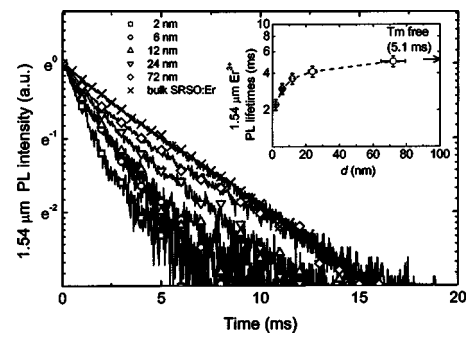


FIG. 3. $1.54 \mu\text{m}$ PL decay traces for alternately doped film and Tm free SRSO: Er film. The deconvoluted 1.54 Er^{3+} PL lifetimes as function of d are summarized in the inset.

doped with Er only is also shown. The Er-only film shows a single-exponential decay with a luminescence lifetime of $\sim 5.1 \text{ m}$. On the other hand, Er and Tm codoped films show nonexponential decay with a fast initial decay followed by a slow tail. As d increases, the fast initial decay is reduced, and the PL decay trace approaches that of the Er-only film. It should be noted, however, that the observed PL decay trace at $1.54 \mu\text{m}$ contains the contribution from the Tm^{3+} luminescence as well. Thus, we deconvoluted the effective $1.54 \mu\text{m}$ Er^{3+} PL lifetimes as follows. First, the Tm^{3+} PL decay at $1.78 \mu\text{m}$ was measured, and confirmed to show a single exponential decay behavior with a decay time of $\sim 400 \mu\text{s}$ from all films, in agreement with previous results (data not shown).¹⁰ Second, the PL decay trace at $1.54 \mu\text{m}$ was integrated to obtain an effective luminescence lifetime. Finally, the Tm^{3+} effective lifetime, scaled by the relative Tm^{3+} PL intensity at $1.54 \mu\text{m}$, was subtracted to obtain the effective Er^{3+} luminescence lifetime. We find that the effective Er^{3+} luminescence lifetime increases from 1.8 to 4.9 m as d is increased from 2 to 72 nm , as is shown in the inset.

The results of Figs. 2 and 3 are in agreement with our previous report that excited Er^{3+} and Tm^{3+} ions interact via a cooperative-upconversion process in which an excited Er^{3+} atom decays nonradiatively by resonantly exciting an excited Tm^{3+} ion from the 3F_4 to the 3H_4 state. The increase in the Er^{3+} with increasing layer thickness therefore indicates that the Tm^{3+} -induced quenching of Er^{3+} luminescence can be suppressed by spatial separation between Er^{3+} and Tm^{3+} , consistent with previous reports that such interaction between RE ions can be described by resonant dipole–dipole transition.^{11,12}

Therefore, we model the energy transfer rate a between Er^{3+} ions at depth of x and Tm^{3+} ions at depth of y as $a = k/(x-y)^6$, where k is a proportionality factor [see Fig. 4(a)]. Experimentally, however, we can only observe the average interaction. Since the RE ions are confined within their respective layers, we calculate average Er–Tm energy transfer rate, a_{ave} , as a function of d by integrating for each layers and then summing over all doped layers as

$$a_{\text{ave}}(d) = k \frac{\sum_{l=1}^m \sum_{n=1}^m \int_{2(l-1)d+\epsilon}^{(2l-1)d-\epsilon} \int_{(2n-1)d+\epsilon}^{2nd-\epsilon} \frac{1}{(x-y)^6} dx dy}{\sum_{l=1}^m \sum_{n=1}^m \int_{2(l-1)d+\epsilon}^{(2l-1)d-\epsilon} \int_{(2n-1)d+\epsilon}^{2nd-\epsilon} dx dy}, \quad (1)$$

where l and n is layer index for Er and Tm doped layer, and m is total number of each RE doped layer [$m = d_{\text{Tot}}/(2d)$]. In

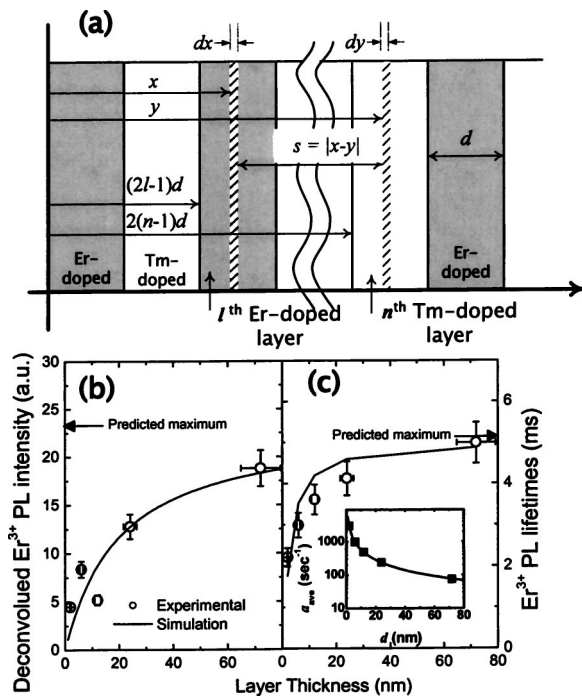


FIG. 4. (a) Schematic explanation for Eq. (1). The comparison between experimental data (open circles) and simulated results (solid lines) of doping layer thickness dependence of (b) deconvoluted Er^{3+} PL intensity and (c) Er^{3+} PL lifetimes. The inset of (c) is the predicted values of a_{ave} .

order to avoid divergence of integral at $x=y$, we need to assume a lower limit of integration, 2ϵ , representing the minimum distance between RE ions. The value of 0.1 nm for ϵ was found to lead to best results, and was used. It was confirmed, however, that the value of ϵ did not significantly affect the result as long as $\epsilon \ll d$.

Equation (1) was then solved analytically with a help from a computation program, and used to simulate the d dependence of the Er^{3+} PL intensity and luminescence lifetime. Previously,¹⁰ we have shown that given an Er-Tm energy transfer rate a , the Er^{3+} PL intensity can be written as

$$I_{\text{Er}}(d) = bN_0 \frac{g}{g + 1/\tau_{\text{Er}}^* + a} W_R, \quad (2)$$

where b , N_0 , g , τ_{Er}^* , and W_R are a proportional factor, the total number of optically active Er^{3+} ions, Er^{3+} excitation rate, Er^{3+} PL lifetime without coupling with Tm^{3+} , and radiative Er^{3+} decay rate, respectively, while the effective 1.54 μm Er^{3+} PL decay lifetime can be written as

$$\tau_{\text{Er}}(d) = \int_0^\infty \exp\left\{-\frac{t}{\tau_{\text{Er}}^*} + a\tau_{\text{Tm}}\left[1 - \exp\left(-\frac{t}{\tau_{\text{Tm}}}\right)\right]\right\} dt. \quad (3)$$

In the present case, a must be replaced by $a_{\text{ave}}(d)$, evaluated using Eq. (1). For numerical simulation, g was evaluated by subtracting the Er^{3+} PL decay rate from the Er^{3+} PL decay rate, and found to be 100 s^{-1} (data now shown). For τ_{Er}^* and τ_{Tm} , the values of 5.1 ms and 400 μs obtained from Fig. 3 were used. Thus, the only adjustable fitting parameters for both Eqs. (2) and (3) were k and bN_0 .

The result of fitting Eqs. (2) and (3) to the measured d dependence of Er^{3+} PL intensity and lifetimes are shown in Figs. 4(b) and 4(c), respectively. The symbols are experimental data, and the solid line is the result of the fit. The

value of k used for fit was $0.26 \text{ nm}^6 \text{ s}^{-1}$. The resulting calculated values of $a_{\text{ave}}(d)$ used in the fits are given in the inset of Fig. 4(c). We obtain good fits to both sets of data using a single set of values for k and bN_0 , indicating the validity of the resonant dipole-dipole interaction model between Er^{3+} and Tm^{3+} , and confirming that by separating the Er^{3+} and Tm^{3+} ions in nm-thin layers, the energy transfer rate a can be reduced from $\sim 5 \times 10^3$ to 70 s^{-1} to increase the Er^{3+} PL efficiency. We note that the value of $\sim 5 \times 10^3$ for a is comparable to the value of $\sim 2 \times 10^3$ we reported previously for Er-Tm coimplanted film, demonstrating the universality of the model. The higher value obtained in the present study is also consistent with the higher Tm^{3+} concentration used in the present study.

Clearly, the Er^{3+} - Tm^{3+} interaction will decrease further with further increase in the layer thickness, up to the limit of a single Er^{3+} - and Tm^{3+} -doped layer. Such a macroscopically inhomogeneous film, however, may be inappropriate for optical amplifier applications as it can lead to different mode profiles for Er^{3+} and Tm^{3+} bands, as well as require complicated pumping schemes to maintain pump uniformity across the amplification band. On the other hand, we note that at a layer thickness of 72 nm the Er^{3+} PL intensity reaches 81% of the maximum value possible without any interaction with Tm^{3+} . Similarly, the value of τ_{Er} for the film with d of 72 nm (4.9 ms) is very close to the value for Tm free Er-doped SRSO film (5.1 ms), indicating near complete recovery of the Er^{3+} luminescence efficiency. Yet since 72 nm is still less than one-tenth of the signal wavelength, the entire film may still be described as being optically homogeneous.

In conclusion, we have investigated controlling the Er^{3+} - Tm^{3+} interaction in Er^{3+} and Tm^{3+} codoped silicon-rich silicon oxide via nm-scale spatial separation. We find that by separating Er^{3+} and Tm^{3+} into nm-thin layers, we can nearly completely suppress Er^{3+} - Tm^{3+} interaction while still maintaining optical homogeneity, thereby obtaining efficient rare earth luminescence across the entire 1.5–2.0 μm wavelength range. The data are well-explained by a model assuming a dipole-dipole interaction between excited Er^{3+} and Tm^{3+} ions, and suggest the possibility of developing compact, ultrawideband optical amplifier employing a single pump source.

This work was supported in part by NRL Project from MOST.

¹L. Pavesi, S. Gaponenko, and L. dal Negro, *Towards the First Silicon Laser*, NATO Science Series II 93.

²M. Fujii, M. Yoshida, Y. Kanzawa, S. Hayashi, and K. Yamamoto, *Appl. Phys. Lett.* **71**, 1198 (1997).

³G. Franzò, D. Pacifici, V. Vinciguerra, and F. Priolo, *Appl. Phys. Lett.* **76**, 2167 (2000).

⁴S.-Y. Seo and J. H. Shin, *Appl. Phys. Lett.* **78**, 2709 (2001).

⁵P. G. Kik, M. L. Brongersma, and A. Polman, *Appl. Phys. Lett.* **76**, 2325 (2000).

⁶P. G. Kik and A. Polman, *J. Appl. Phys.* **91**, 534 (2001).

⁷A. J. Kenyon, C. W. Pitt, T. Shimizu-Iwayama, D. E. Hole, N. Sharma, and C. J. Humphreys, *J. Appl. Phys.* **91**, 367 (2002).

⁸H.-S. Han, S.-Y. Seo, J. H. Shin, and N. Park, *Appl. Phys. Lett.* **81**, 3720 (2002).

⁹J. Lee, J. H. Shin, and N. Park, *Post Deadline Papers on Optical Fiber Conference 2004*, PDP19, Los Angeles 2004.

¹⁰S.-Y. Seo, J. H. Shin, B.-S. Bae, N. Park, J. J. Penninkhof, and A. Polman, *Appl. Phys. Lett.* **82**, 3445 (2003).

¹¹E. Snoeks, P. G. Kik, and A. Polman, *Opt. Mater. (Amsterdam, Neth.)* **5**, 159 (1996).

¹²M. J. Weber, *Phys. Rev. B* **4**, 2932 (1971).